RESEARCH PAPER

PCCP
www.rsc.org/pccp

Small angle neutron scattering and viscosity studies of micellar solutions of bis-cationic surfactants containing hydroxyethyl methyl quaternary ammonium head groups

Mahendra Borse,[a] Vikas Sharma,[a] V. K. Aswal,[b] Naveen K. Pokhriyal,[c] Jayant V. Joshi,[c] Prem S. Goyal[c] and Surekha Devi*[a]

[a] *Department of Chemistry, Faculty of Science, M.S. University of Baroda, Vadodara 390 002, Gujarat, India. E-mail: surekha_devi@yahoo.com; Fax: +91-265-2795569/2791891; Tel: +91-265-2795552*
[b] *Solid State Physics Division, Bhabha Atomic Research Centre, Trombay, Mumbai 400 085, India*
[c] *Inter University Consortium for DAE Facilities, Bhabha Atomic Research Centre, Trombay, Mumbai 400 085, India*

Received 23rd February 2004, Accepted 13th April 2004
First published as an Advance Article on the web 21st May 2004

The effect of head group polarity and spacer chain length of bis-cationic surfactants on shape, size and rheology of surfactant aggregates in aqueous solution has been investigated through small angle neutron scattering (SANS) and viscosity measurements. A series of bis-cationic surfactants $C_{12}H_{25}N^+(CH_3)(C_2H_4OH)$–$(CH_2)_s$–$N^+(CH_3)(C_2H_4OH)C_{12}H_{25}$ $2Br^-$, referred to as 12-s-12 MEA, where two highly polar quaternary amine centers are covalently connected through polymethylene spacers at head group level, has been synthesized and characterized. Critical micellar concentration of these surfactants in aqueous solution determined by tensiometry and conductometry was observed to be 10–100 times lower than conventional bis-cationic surfactants [$C_{12}H_{25}N^+(CH_3)_2$–$(CH_2)_s$–$N^+(CH_3)_2C_{12}H_{25}$ $2Br^-$, referred to as 12-s-12 DMA]. The extent of aggregate growths and variation in shape and size of micelles was observed to be strongly dependent upon head group polarity, spacer chain length and experimental conditions such as concentration and temperature.

1. Introduction

Surfactant molecules above critical micellar concentration (cmc) in aqueous solution are known to form variety of microstructures such as spherical, ellipsoidal, vesicular, rod-like and thread-like.[1–9] The microstructure of surfactant aggregates depends on the molecular architecture of the surfactant and solution conditions, such as concentration and temperature.[1–7] The bis-cationic surfactants where two long chains of ter-amines are covalently attached through the polymethylene spacer chain at the head group level, have recently been well studied.[10–15] The physicochemical properties of bis-cationic surfactant molecules primarily depend upon the structure of molecules under consideration, as seen in more than 10 times decrease in cmc, when two DTAB molecules are covalently connected through polymethylene spacer chain at the head group level.[8,11] Moreover, the microstructure of micelles and physicochemical properties of bis-cationic surfactants depend on the nature and length of the spacer chain which has been examined for different types of spacers such as polymethylene, polyoxyethylene, and aromatic rings in the molecules.[12–18] Zana and co-workers[9,11] studied micellar solutions of conventional bis-cationic surfactants 12-s-12 DMA through cryo-transmission electron microscopy. They have reported that surfactants with spacer chain length 2 and 3 show long thread-like micelles, while nearly spherical micelles are formed with spacer chain length 4 and 6. SANS studies of alkanediyl-α,ω-bis(alkyldimethylammonium bromide) bis-cationic surfactants containing –$N(CH_3)_2$ head groups and C_{10}, C_{16} alkyl chain lengths have been extensively reported.[12–15,19] However, this is a first attempt to examine the effect of variation in head polarity along with spacer length on physicochemical properties and microstructure of bis-cationic surfactant aggregates. We report the synthesis, characterization and physicochemical properties of a series of novel 12-s-12 MEA bis-cationic surfactants, where the polarity of head groups of conventional 12-s-12 DMA bis-cationic surfactants has been altered by replacing –$N(CH_3)_2$ head groups by –$N(CH_3)(C_2H_4OH)$ groups. Small-angle neutron scattering and viscosity measurements have been used to study the microstructure and rheology of these novel series of bis-cationic surfactants.

2. Experimental

2.1 Materials

n-Dodecyl bromide, α,ω-dibromoalkane and 2(methylamino)-ethanol were purchased from Lancaster Chemical Company, Morecambe, England. *N*,n-dodecyl hydroxyethylmethyl amine was prepared by refluxing n-dodecyl bromide with 2(methylamino)ethanol in dry ethanol at 80 °C for 15 h. All the reagents and solvents used were of AR grade. The identity of intermediate compound was confirmed by elemental, FTIR and ^1H NMR analysis. Triple distilled deionized water was used for all physicochemical measurements.

2.2 Synthesis of dimeric surfactants

The dimeric surfactants were synthesized by refluxing 2.2 moles of dodecyl hydroxyethylmethyl amine in dry acetone

DOI: 10.1039/b402767c

with 1.0 mole of α,ω-dibromo alkane for 70 h, at 60 °C.

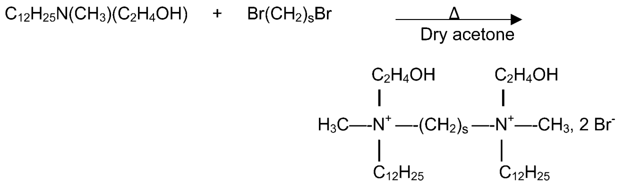

$$C_{12}H_{25}N(CH_3)(C_2H_4OH) + Br(CH_2)_sBr \xrightarrow[\text{Dry acetone}]{\Delta} H_3C\text{—}\overset{C_2H_4OH}{\underset{C_{12}H_{25}}{N^+}}\text{—}(CH_2)_s\text{—}\overset{C_2H_4OH}{\underset{C_{12}H_{25}}{N^+}}\text{—}CH_3,\ 2\,Br^-$$

The solvent from reaction mixture was removed under vacuum and the crude white solid thus obtained was purified by washing with hexane/ethyl acetate mixture and recrystallized from acetone/methanol mixture for at least three times to obtain pure compound. The overall yield of the surfactant was observed to be 70–80%. The identity and purity of the final product was confirmed by TLC, elemental, FTIR and ^{1}H NMR analysis.

2.3 Conductance measurements

The critical micellar concentration of the surfactants was measured through conductance measurements at 30.0 ± 0.1 °C, using Digital Conductivity Meter (Equip-Tronics, Model No.-664). The conductance of different solutions was measured on addition of an aliquot of a known concentration of a surfactant solution to a given volume of the thermostated solvent. The average degree of ionization (α_{ave}) of a micelle was taken as the ratio of the values of $\mathrm{d}k/\mathrm{d}C$ above and below the cmc.

2.4 Surface tension measurements

The reduction in the surface tension of water with respect to surfactant concentration was measured on du-Noüy tensiometer (Winson and Co. Kolkata, India). The cmc values were obtained from inflection point in the plots of the surface tension (γ) against log concentration (C).

2.5 Viscosity measurements

Viscometry can be used to obtain gross structural information of the surfactant solutions.[20–23] The absolute viscosity values of aqueous surfactant solutions were determined as a function of shear rate, temperature, surfactant concentrations and spacer chain length, using Brook Field DV-III digital cone and plate rheometer. The diameter of the cone was 40 mm and the cone angle was 0.8°. To ensure the reproducibility of the measurements, great care was exercised when the sample was introduced into the rheometer to avoid shear effect on the solution. Measurements were repeated (2–3 times) on fresh solutions and were found to be reproducible within 5%. The measuring device was equipped with a Peltier Plate temperature unit for good temperature control over an extended time.

2.6 SANS measurements

Small angle neutron scattering is a powerful technique for studying the shape and size of surfactant aggregates in aqueous solutions.[24] Small-angle neutron scattering measurements for 12-s-12 MEA bis-cationic surfactants, where s = 4, 6, 8 and 10 were carried out using SANS diffractometer at Dhruva reactor, Bhabha Atomic Research Center (BARC), Mumbai, India. The surfactant solutions used for SANS studies were prepared in D_2O, obtained from Heavy Water Division of BARC. The use of D_2O instead of H_2O provides very good contrast between surfactant aggregates and solvent in a SANS experiment. The sample-to-detector distance was 1.85 m for all the runs. The spectrometer makes use of a BeO filtered beam and has a resolution ($\Delta Q/Q$) of about 30% at $Q = 0.05$ Å^{-1}. The angular distribution of the scattered neutrons was recorded using one-dimensional position-sensitive detector (PSD). The range of wave vector transfer Q of the instrument was 0.018–0.30 Å^{-1} and is given as $4\pi\sin\theta/\lambda$, where λ is the wavelength of the incident neutron and 2θ is the scattering angle. The detector allows a simultaneous recording of data over the full Q range. The wavelength of incident neutron (λ) was 0.52 nm. The solutions were held in a 0.5 cm path length UV grade quartz sample holder with tight fitting teflon stoppers sealed with para-film. In most of the measurements the surfactant concentration was 100 mM and the sample temperature was 30 ± 0.1 °C. The effect of the concentration on the microstructure of 12-4-12 MEA bis-cationic surfactant in aqueous solution at 30 °C was studied in the concentration range of 50 to 100 mM. The effect of temperature variations on the microstructure of the micelle was investigated for 12-4-12 MEA surfactant solution of 100 mM concentration at 30, 40 and 60 °C. The measured scattering intensities of neutron were corrected for background, empty cell scattering and sample transmission. The intensities then were normalized to absolute cross-section units. Thus plots of $\mathrm{d}\Sigma/\mathrm{d}\Omega$ *vs.* Q were obtained. The uncertainty in the measured scattering intensities is estimated to be <10%. The experimental points are fitted using a nonlinear least square method.

3. SANS data analysis

In SANS one measures the differential scattering cross-section per unit volume ($\mathrm{d}\Sigma/\mathrm{d}\Omega$) as a function of the scattering vector Q. For a system of charged interacting micelles $\mathrm{d}\Sigma/\mathrm{d}\Omega$ is given by[24–27]

$$\frac{\mathrm{d}\Sigma}{\mathrm{d}\Omega} = n(\rho_{\mathrm{m}} - \rho_{\mathrm{s}})^2 V^2 \left[\left\langle F(Q)^2 \right\rangle + \langle F(Q)\rangle^2 (S(Q) - 1)\right] + B \qquad (1)$$

where n denotes the number density of the micelles, ρ_{m} and ρ_{s} are, respectively, the scattering length densities of the micelle and the solvent and V is the volume of the micelle. The aggregation number N of the micelle is related to the micellar volume V by the relation $V = Nv$, where v is the volume of the surfactant monomer. The volume of the 12-s-12 MEA monomer including the head groups was calculated by using an equation $v = (947 + 26.9\ \mathrm{s})$ Å^3, derived from Tanford's formula. $F(Q)$ is the single particle form factor and $S(Q)$ is the interparticle structure factor. B is a constant term that represents the incoherent scattering background, which is mainly due to hydrogen in the sample. The single particle form factor $F(Q)$ has been calculated by treating the micelle as a prolate ellipsoid.[28] For such an ellipsoidal micelle

$$\left\langle F^2(Q)\right\rangle = \int_0^1 \left[F(Q,\mu)^2 \mathrm{d}\mu\right] \qquad (2)$$

$$\langle F(Q)\rangle^2 = \left[\int_0^1 F(Q,\mu)\mathrm{d}\mu\right]^2 \qquad (3)$$

$$F(Q,\mu) = \frac{3(\sin x - x\cos x)}{x^3} \qquad (4)$$

$$x = Q[a^2(1-\mu^2) + b^2\mu^2)]^{1/2} \qquad (5)$$

where a and b are, respectively, the semiminor and semimajor axes of the ellipsoidal micelle and μ is the cosine of the angle between the axis of resolution and the wave vector transfer Q.

In general, micellar solutions of ionic surfactants show a correlation peak in the SANS distribution.[27,28] The peak arises because of the corresponding peak in the interparticle structure factor $S(Q)$ and indicates the presence of electrostatic interactions between the micelles. $S(Q)$ specifies the correlation between the centers of different micelles and it is Fourier transform of the radial distribution function $g(r)$ for the mass centers of the micelles. We have calculated $S(Q)$ as derived by Hayter and Penfold[25,26] from the Ornstein–Zernike equation and using the rescaled mean spherical approximation. The micelle is assumed to be a rigid equivalent sphere of diameter $\sigma = 2(a^2b)^{1/3}$ interacting through a screened Coulomb potential, which is given by

$$u(r) = u_0\sigma\frac{\exp[-\kappa(r-\sigma)]}{r}, \quad r > \sigma \tag{6}$$

where κ is the Debye–Hückel inverse screening length and is calculated by

$$\kappa = \left[\frac{8\pi N_A e^2 I}{10^3 \varepsilon k_B T}\right]^{1/2} \tag{7}$$

where I is the ionic strength of the micellar solution and is determined from the CMC and dissociated counterions of the micelles. The fractional charge α $(= Z/N$, where Z is the micellar charge) is the charge per surfactant molecule in the micelle. The contact potential u_0 is given by

$$u_0 = \frac{Z^2e^2}{\pi\varepsilon\varepsilon_0\sigma(2+\kappa\sigma)^2} \tag{8}$$

where ε is the dielectric constant of the solvent medium, ε_0 is the permittivity of free space and e is the electronic charge.

Although micelles may produce polydisperse systems, we have assumed them as monodisperse for the simplicity of the calculation and to limit the number of unknown parameters in the analysis. The dimensions of the micelle, aggregation number and the fractional charge have been determined from the analysis. The semi-major axis (b), semi-minor axis (a) and the fractional charge (α) are the parameters optimized by means of a nonlinear least squre fitting program while analyzing the SANS data. The aggregation number is calculated by using the relation $N = 4\pi a^2 b/3v$, where v is the volume of the surfactant monomer.

4. Results and discussion

4.1 Characterization

The structure and purity of synthesized series of bis-cationic surfactants was confirmed through FTIR, elemental, and ^{1}H NMR analysis.

The IR spectra of the surfactants were recorded in KBr pellets using Perkin Elmer FTIR spectrophotometer RX, of a resolution 2 cm^{-1}. The absorption bands were observed at 3401–3656 cm^{-1} (OH stretching), 2916 cm^{-1} (CH stretching), 1108 cm^{-1} (CN stretching), 1084 cm^{-1} (CO stretching) and 720 cm^{-1} (CH rocking of long alkyl chain).

Elemental analysis and ^{1}H NMR spectra of products in $CDCl_3$ were determined using Perkin Elmer Series II elemental analyzer and 300 MH$_Z$ Bruker NMR spectrophotometer, respectively.

Butanediyl-1,4,-*N*,*N*′-bis(dodecyle hydroxyethyl methyl ammonium bromide). Represented as (12-4-12 MEA) M.P. 195 ± 2 °C; C, H, N analysis. Calculated for $C_{34}H_{74}N_2O_2Br_2$ was C: 58.10; H: 10.61; N: 3.98%. Found C: 58.20; H: 10.75; N: 4.01%. ^{1}H NMR analysis, δ 0.84 ppm (t, 6H $2CH_3$ alkyl chain), 1.25–1.40 ppm (br m, 36 H, $18CH_2$ alkyl chain), 1.75 ppm (m, 4H, $2CH_2$ alkyl chain), 2.1 ppm (m, 4H, $2CH_2$ spacer chain), 3.25 ppm (s, 6H, $2N^+CH_3$), 3.62 ppm (t, 12 H, $2\times N^+(CH_2)_3$), 3.82 ppm (t, 4H, $2CH_2$-OH) and 4.18 ppm (s, 2H, 2OH).

Hexanediyl-1,6-*N*-*N*′-bis(dodecyl hyroxyethyl methyl ammonium bromide). Represented as (12-6-12 MEA) M.P. 206 ± 2 °C; C, H, N analysis. Calculated for $C_{36}H_{78}N_2O_2Br_2$ was C: 59.16; H: 10.75; N: 3.83%. Found C: 59.49; H: 10.86; N: 4.00%. ^{1}H NMR analysis, δ 0.84 ppm (t, 6 H, $2CH_3$ alkyl chain), 1.25 ppm (br m, 40 H, 20 CH_2 alkyl chain), 1.65 ppm (m, 4 H, $2CH_2$ spacer chain), 1.95 ppm (m, 4 H, $2CH_2$ spacer chain), 3.25 ppm (s, 6 H, $2N^+CH_3$), 3.59 ppm (t, 12 H, $2N^+(CH_2)_3$), 3.75 ppm (t, 4 H, $2CH_2$-OH), 4.15 ppm (s, 2 H, 2OH).

Octanediyl-1,8-*N*-*N*′-bis(dodecyl hydroxyethyl methyl ammonium bromide). Represented as (12-8-12 MEA)M.P.193 ± 2 °C; C, H, N analysis. Calculated for $C_{38}H_{82}N_2O_2Br_2$ was C: 60.14; H: 10.89; N: 3.69%. Found C: 60.32; H: 11.00; N: 3.73%. ^{1}H NMR analysis, δ 0.81 ppm (t, 6 H, $2CH_3$ alkyl chain), 1.17 ppm (br m, 40 H, $20CH_2$ alkyl chain), 1.35 ppm (t, 8 H, $4CH_2$ spacer chain), 1.74 ppm (m, 4 H, $2CH_2$ spacer chain), 3.20 ppm (s, 6 H, $2N^+CH_3$), 3.59 ppm (t, 12 H, $2N^+(CH_2)_3$), 3.93 ppm (t, 4 H, $2CH_2$-OH), 3.99 ppm (s, 2 H, 2OH).

Decanediyl-1,10-*N*-*N*′-bis(dodecyl hydroxyethyl methyl ammonium bromide). Represented as (12-10-12 MEA) M.P. 203 ± 2 °C; C, H, N analysis. Calculated for $C_{40}H_{86}N_2O_2Br_2$ was C: 61.05; H: 11.02; N: 3.56%. Found C: 61.25; H: 11.10; N: 3.60%. ^{1}H NMR analysis, δ 0.81 ppm (t, 6 H $2CH_3$ alkyl chain), 1.30 ppm (m, 40 H, $20CH_2$ alkyl chain),1.35 ppm (t, 8 H, $4CH_2$ spacer chain), 1.70 ppm (m, 8 H, $4CH_2$ spacer chain), 3.24 ppm (s, 6 H, $2N^+CH_3$), 3.67 ppm (t, 12 H, $2\times N^+(CH_2)_3$), 4.05 ppm (t, 4 H, $2CH_2$-OH), 5.12 ppm (s, 2 H, 2OH).

4.2 Critical micellar concentration

The cmc values for 12-s-12 MEA novel series of bis-cationic surfactants were determined by surface tension and conductance measurements. The cmc values obtained from both the techniques show a similar trend with spacer chain length and are given in Table 1. It is interesting to note that cmc data of the 12-s-12 MEA bis-cationic surfactants are observed to be 10–100 times lower than the conventional 12-s-12 DMA bis-cationic surfactants.[9–10] For 12-s-12 MEA, hydrogen bonding with water can take place through oxygen atom of $-C_2H_4OH$ groups. This is likely to provide additional hydration at the head group level resulting in screening of Coulombic forces of repulsion between charged heads and helping

Table 1 Critical micellar concentration (cmc), average degree of ionization (α_{ave}) and Gibb's free energy of micellization (ΔG_m) for 12-s-12 MEA novel series of bis-cationic surfactants, at 30 °C[a]

Spacer length (s)	cmc by conductometry $C \times 10^{-5}$ M	cmc by tensiometry $C \times 10^{-5}$ M	(α_{ave})	(ΔG_m) kJ mol^{-1}
4	3.49 ± 0.10 (117 ± 10)	2.78 ± 0.10	0.26 (0.31)	−32.06
6	4.49 ± 0.10 (103 ± 10)	4.33 ± 0.10	0.31 (0.33)	−30.01
8	3.99 ± 0.15 (83 ± 10)	3.18 ± 0.10	0.36 (0.45)	−29.01
10	3.12 ± 0.10 (63 ± 10)	2.59 ± 0.10	0.39 (0.54)	−29.01

[a] The values given in brackets are of conventional 12-s-12 DMA bis-cationic surfactants with $-N^+(CH_3)_2$ head groups, taken from ref. 8.

12-s-12 MEA surfactants to form aggregates at a lower concentration than those of 12-s-12 DMA surfactants.

Fig. 1 shows that cmc goes on increasing up to the spacer chain length of 6 carbon atoms and thereafter decreases with increase in the spacer length. Similar behavior has also been reported by Zana and coworkers.[8,9] The variation in cmc values with the spacer chain length can be attributed to the conformational changes taking place at the polymethylene spacer. For the spacer chain $s \leq 6$, spacer remains in a fully extended conformation making it somewhat difficult to be located at micelle-water interface, whereas for longer spacers $s > 6$, spacer tries to form a loop in the hydrophobic core of the micelle disrupting the micelle geometry. This statement is well supported by theoretically as well as experimentally calculated distances (*d*) between the charged heads of the surfactant molecule (Table 3). The observed increasing difference between the theoretical and experimental values of the equilibrium distance between charged heads shows increased tendency of formation of a loop due to the hydrophobic nature of a spacer.

The overall average degree of ionization (α_{ave}) of micelle was observed to be less than that of conventional bis-cationic surfactants and increases with increasing the spacer chain length, as shown in Table 1. The Gibb's free energy of micellization (ΔG_m) was obtained from conductance measurement and is given in Table 1. The observed more negative ΔG_m value for 12-4-12 MEA shows more favorable micellization than the surfactant with spacer length of 6, 8 and 10.

4.3 Viscosity of micellar solutions

Table 2 shows the viscosity data for 100 mM, 12-s-12 MEA bis-cationic surfactants with different spacer lengths. Surfactant with spacer length 4 showed very high absolute viscosity in comparison with the surfactant with spacer lengths 6, 8 and 10, indicating the formation of larger aggregates in aqueous solution. Fig. 2 shows the effect of the shear rate on viscosity behavior as a function of spacer length, and it was observed that all the present surfactants show essentially Newtonian behavior. Table 2, shows the viscosity at various concentrations and temperatures for surfactant with spacer length of 4 carbon atoms. As expected, the viscosity decreases with decreasing the surfactant concentration or increasing the temperature.

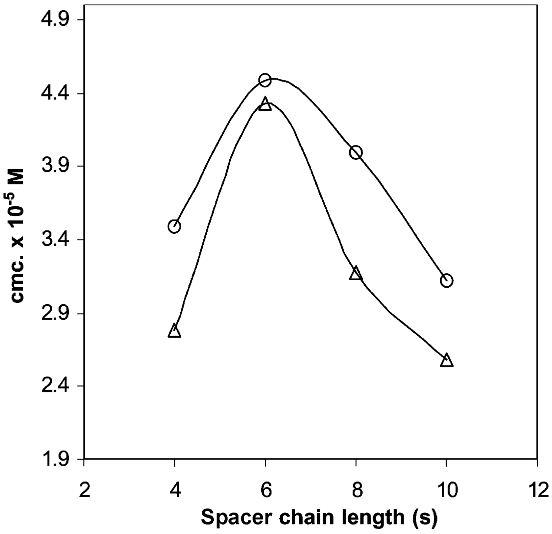

Fig. 1 Effect of the spacer chain length on the critical micellar concentration of 12-s-12 MEA novel series of bis-cationic surfactants at 30 °C. Variation in the cmc values as a function of spacers chain length, by tensiometry (△) and by conductometry (○).

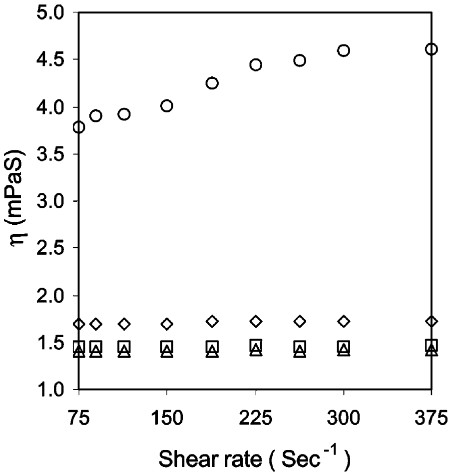

Fig. 2 Effect of variation of shear rate on absolute viscosity of 12-s-12 MEA novel series of bis-cationic surfactants at 100 mM and 30 °C. s = 4 (○), 6 (△), 8 (□),10 (◇).

4.4 SANS and micellar solutions

In the SANS experiment, a beam of neutrons is directed upon the sample under examination and the neutron scattering intensities in different directions are measured. Since the neutrons are scattered by the nuclei in the sample, even isotopes of the same element can differ in their scattering power. Thus, by taking aggregates in D_2O rather than in H_2O, the scattering densities of various regions can be obtained, since deuterons and protons differ widely in their respective scattering capacities. SANS is one of the powerful techniques for getting the structural information especially on micellar aggregates.[24]

Effect of spacer chain length on surfactant aggregates. To understand the effect of the head group polarity and spacer chain length on the microstructure of surfactant aggregates in aqueous solution, SANS measurements were carried out at 100 mM solution of 12-s-12 MEA surfactant with spacers (s) = 4, 6, 8 and 10. SANS distributions (Fig. 3) show well defined correlation peaks irrespective of the spacer chain length, due to a peak in the inter-micellar structure factor $S(Q)$. The correlation peaks appears at around $Q_{max} \sim 2\pi/D$, where D is the average distance between the micelles. Since

Table 2 Effect of spacer lengths, concentrations and temperatures on the absolute viscosity of 12-s-12 MEA novel series of bis-cationic surfactants in aqueous solutions

Parameter	η/m PaS
Effect of the spacer chain length(s) on the absolute viscosity of 12-s-12 MEA bis-cationic surfactants, at 100 mM and 30 °C	
s = 4	4.60 ± 0.20
s = 6	1.42 ± 0.07
s = 8	1.47 ± 0.07
s = 10	1.72 ± 0.09
Effect of the concentrations on the absolute viscosity for 12-4-12 MEA bis-cationic surfactant, at 30 °C	
100 mM	4.60 ± 0.20
75 mM	1.70 ± 0.09
50 mM	1.22 ± 0.06
25 mM	1.07 ± 0.05
Effect of the temperature on the absolute viscosity for 12-4-12 MEA bis-cationic surfactant, at 100 mM	
30 °C	4.60 ± 0.20
35 °C	2.44 ± 0.12
40 °C	1.92 ± 0.10
45 °C	1.60 ± 0.08

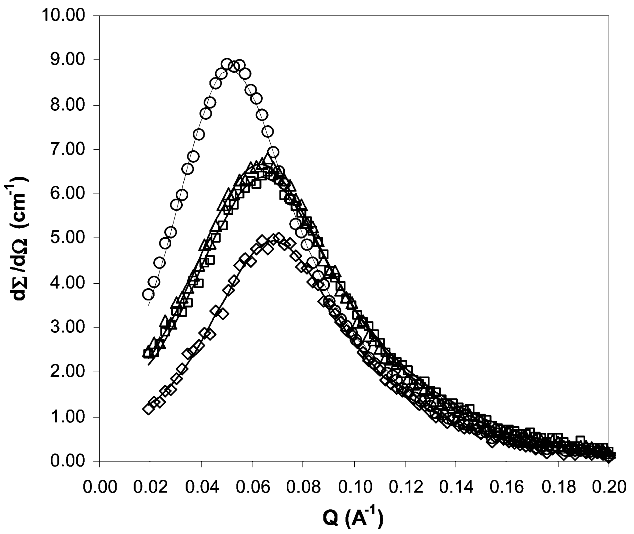

Fig. 3 Effect of spacer chain length on the SANS distribution for 12-s-12 MEA novel series of bis-cationic surfactants at 100 mM concentrations and 30 °C. The solid line shows the theoretical fits and the symbols are experimentally determined values. s = 4 (○), 6 (△), 8 (□), 10 (◇).

$Q_{\max}$ was found to vary with spacers, one can conclude that the number density (n) of micelles is not the same in the above sample even when they have identical surfactant concentration. It is observed from Fig. 3 that the peak positions shift towards higher Q values with increase in the spacer chain length from 4 to 6. However, the shift in Q is small with the change in spacer chain length from 6 to 10. The observed SANS data were analyzed by taking aggregation number (N), effective fractional charge (α) and semi-minor axis (a) as fitting parameters and semi-major axis (b) is calculated by using equation $b = (3N\nu/4\pi a^2)$. The extracted micellar parameter values are given in Table 3. The equilibrium distances between the charged heads (d) calculated for the bis-cationic surfactants with respect to spacer length are given in Table 3. From the results in Table 3, the aggregation number (N) was observed to decrease significantly and fractional charge per monomer was observed to increase with spacer length. The observed large variation in values for spacer length 4 to 6 rather than for the spacer length 6 to 10, can be attributed to the conformational changes of spacer at micelle/water interface, as discussed earlier. The observed increase in the equilibrium distance (d) between the charged heads with spacer length increases the spontaneous packing curvature restricting the growth of micelle. The surfactant with shorter spacer of 4 carbon atoms shows larger aggregates in aqueous solution and high viscosity (Table 2 and 3). Zana *et al.*[9,11] have reported spherical micelles for 12-s-12 DMA bis-cationic surfactant with spacer lengths 4 and 6 whereas in the present study the surfactant with change in head polarity 12-s-12 MEA with spacer lengths 4 and 6 shows formation of more elongated ellipsoidal micelles, indicating that the increase in head polarity of surfactant increases the aggregation tendency. The change in the head group polarity and spacer length of the bis-cationic surfactant results in a significant change. We have observed the b/a ratio to decrease from 4.23 to 2.82 with increasing the spacer length from 4 to 10 indicating that the spacer length 4 shows higher tendency of aggregation than larger spacers 6, 8 and 10.

Effect of the concentration on surfactant aggregates. The SANS data from 12-4-12 MEA bis-cationic surfactants at different concentrations and at 30 °C is illustrated in Fig. 4. The concentration range examined was 50 to 100 mM. All distributions were observed to shows well defined correlation peaks because of the intermicellar structure factor $S(Q)$. The correlation peaks appear at around $Q_{\max} \sim 2\pi/D$. It was observed that with increased concentration, there is little shift in the peak position towards higher Q values with overall increase in the peak intensity. With increase in the concentration, the average distance between the micelles decreases indicating an increase in the number density of micelles. The increase in concentration of surfactant helps aggregation growth along the direction of semi-major axis (b) to form more prolate ellipsoidal micelle ($b/a = 4.23$). The effective fractional charge was observed to decrease with increase in the concentration of surfactants from 50 to 100 mM. This can be attributed to the increase in aggregation numbers, which increases the surface charge density of the micelle and helps to increase the association of counterions (Table 4).

Effect of temperature on surfactant aggregates. Fig. 5 shows the SANS distribution for 100 mM of 12-4-12 MEA bis-cationic surfactant at 30, 45, and 60 °C. It is observed that the peak position in SANS shifted to the higher Q values with overall decrease in the peak intensity and increase in the broadness

Table 3 Effect of the spacer chain length (s) on the micellar parameters of 12-s-12 MEA novel series of bis-cationic surfactants of 100 mM at 30 °C[a]

Spacer length (s)	Aggregation number (N)	Effective monomer charge (α)	Semi-minor axis, a (Å)	Semi-major axis, b (Å)	Equilibrium distance between charged heads (d) Å	b/a
4	108 ± 8	0.11 ± 0.01	18.6 ± 0.5	78.6 ± 1.8	7.25 (7.56)	4.23 ± 0.05
6	56 ± 5	0.19 ± 0.01	16.4 ± 0.5	55.3 ± 1.4	8.23 (10.64)	3.32 ± 0.05
8	55 ± 5	0.18 ± 0.01	17.2 ± 0.5	51.3 ± 1.3	8.37 (13.74)	3.01 ± 0.05
10	52 ± 4	0.24 ± 0.01	17.6 ± 0.5	48.7 ± 1.3	8.59 (16.80)	2.82 ± 0.05

[a] The values given in brackets are the theoretically calculated distances between the charged heads (d) of the surfactant molecule.

Table 4 Effect of the variation in concentrations on the micellar parameters of 12-4-12 MEA bis-cationic surfactant at 30 °C

Concentrations (mM)	Aggregation number (N)	Effective monomer charge (α)	Semi-minor axis, a (Å)	Semi-major axis, b (Å)	b/a
100	108 ± 8	0.11 ± 0.01	18.6 ± 0.5	78.6 ± 1.8	4.23 ± 0.05
75	81 ± 6	0.14 ± 0.01	18.3 ± 0.5	60.8 ± 1.5	3.34 ± 0.05
50	63 ± 5	0.17 ± 0.01	17.7 ± 0.5	50.4 ± 1.4	2.78 ± 0.06

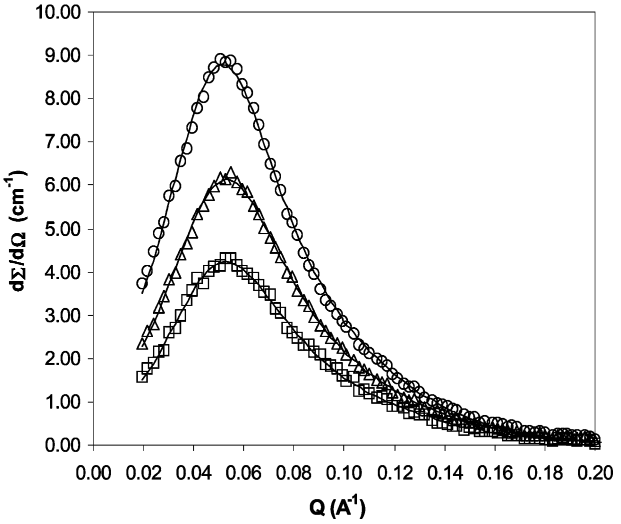

Fig. 4 Effect of variation of concentration on SANS distribution for 12-4-12 MEA bis-cationic surfactant at 30 °C. The solid line shows the theoretical fits and the symbols are experimentally determined values. 100 mM (○), 75 mM (△), 50 mM (□).

of peak, when temperature increased. Similarly, the correlation peak Q_{max} was observed to change with temperature, indicating the increased number density of micelle changes with temperature. The micellar parameters in these systems are given in the Table 5. The increase in temperatures enhances the degree of dissociation of counterions and affects the magnitude of electrostatic repulsion. This results in decrease of the aggregation number (N), upon increase of the temperature. The effective fractional charge was observed to increase with increasing the temperature. Since the smaller effective charge indicates a more ellipsoidal morphology, increasing the temperature appears to induce somewhat ellipsoidal to sphere transition for 12-4-12 MEA. This notation is also supported by the concomitant decrease in b/a *ca.* 4.23 to *ca.* 2.87 upon increase in temperature.

Table 5 Effect of temperatures on micellar parameters of 12-4-12 MEA bis-cationic surfactant at 100 mM concentration

Temperature T (°C)	Aggregation number (N)	Effective monomer charge (α)	Semi-minor axis, a (Å)	Semi-major axis, b (Å)	b/a
30	108 ± 8	0.11 ± 0.01	18.6 ± 0.5	78.6 ± 1.8	4.23 ± 0.05
45	71 ± 4	0.15 ± 0.01	18.2 ± 0.5	53.8 ± 1.4	3.02 ± 0.05
60	57 ± 5	0.21 ± 0.01	17.1 ± 0.5	49.0 ± 1.4	2.87 ± 0.06

5. Conclusion

A series of novel bis-cationic surfactants 12-s-12 MEA where two highly polar quaternary amine centers are covalently connected through polymethylene spacers of 4, 6, 8 and 10 at the head group level, has been synthesized and characterized. To the best of our knowledge, this is a first report on the synthesis of surfactants with quaternary amines with ethanolic groups. The presence of ethanolic groups at the head groups increases the head polarity of the surfactants, resulting in reduction of the cmc, average degree of ionization (α_{ave}) and higher tendency of surfactants to aggregate, as compared to conventional 12-s-12 DMA bis-cationic surfactants containing $-N^{+}(CH_3)_2$ head groups. The cmc of the surfactant increases up to spacer length 6 and then it decreases with further increase in the spacer length. SANS studies show that the size of micelles for spacer length 4 is much larger than those of larger spacer lengths. This is well supported by viscosity measurements as the surfactant with spacer length 4 shows the very high viscosity than those of spacer 6, 8 and 10. The flow curves of all the 12-s-12 MEA surfactants show Newtonian behavior. It has also been found that the size of micelles decreases when the concentration is decreased or the temperature is increased.

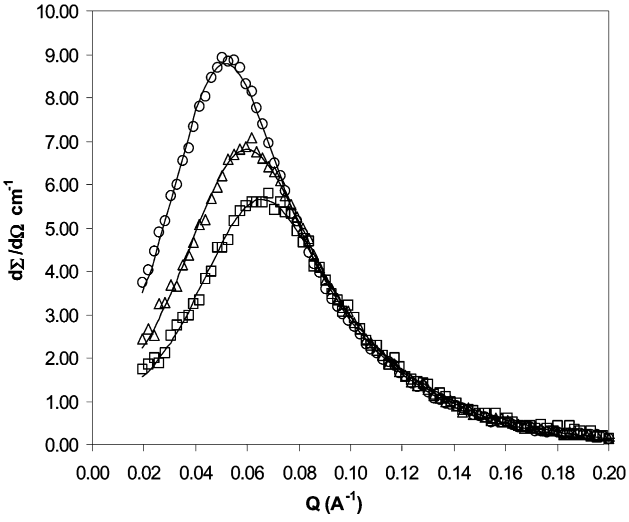

Fig. 5 Effect of temperatures on SANS distribution for 100 mM 12-4-12 MEA bis-cationic surfactant. The solid line shows the theoretical fits and the symbols are experimentally determined values. 30 °C (○), 45 °C (△) and 60 °C(□).

Acknowledgements

We gratefully acknowledge the financial support for this work from the Department of Science and Technology, New Delhi and IUC-DAEF Mumbai Center. Initial help extended in the synthesis of surfactants by Dr Alpesh Patel is gratefully acknowledged.

References

1 H. Wennerstrom and B. Lindman, *Phys. Rep.*, 1979, **52**, 1.
2 F. M. Menger, *Angew Chem., Int. Ed. Engl.*, 1991, **30**, 1086.
3 C. A. Bunton, L. Robinson, J. Schaak and M. F. Stern, *J. Org. Chem.*, 1971, **36**, 2346.
4 P. K. Vinson, J. R. Bellare, H. T. Davis, W. G. Miller and L. E. Scriven, *J. Colloid Interface Sci.*, 1991, **74**, 91.
5 J. Appell, G. Port, A. Khatory, F. Kem and S. J. Candau, *J. Phys. (Paris)*, 1992, **2**, 1045.
6 H. Hirata, M. Sato, Y. Sakaiguchi and Y. Katsube, *Colloid Polym. Sci.*, 1988, **266**, 862.
7 D. A. Jaeger, B. Li and T. Jr. Clark, *Langmuir*, 1996, **12**, 4314.
8 R. Zana, M. Benrroau and R. Rueff, *Langmuir*, 1991, **76**, 1072.
9 R. Zana and Y. Talmon, *Nature (London)*, 1993, **362**, 228.
10 D. Danino, Y. Talmon and R. Zana, *Langmuir*, 1995, **11**, 1448.
11 R. Zana, *Structure–Performance Relationship in Surfactants*, ed. K. Esumin and M. Ueno, Surfactant Science Series, M. Dekker, New York, 1997, vol. 70, ch. 6, and references therein.
12 X. Wang, J. Wang, H. Yan, P. Li and R. K. Thomas, *Langmuir*, 2004, **19**, 53.
13 S. De, V. K. Aswal, P. S. Goyal and S. Bhattacharya, *J. Phys. Chem.*, 1996, **100**, 11 664.
14 S. D. Wettig, X. Li and R. E. Verrall, *Langmuir*, 2003, **19**, 3666.
15 S. D. Wettig, P. Nowak and R. E. Verrall, *Langmuir*, 2002, **18**, 5354.
16 H. Hirata, N. Hattori, M. Ishida, H. Okabayashi, M. Frusaka and R. Zana, *J. Phys. Chem.*, 1995, **99**, 17 778.
17 R. Zana, *Adv. Colloid Interface Sci.*, 2002, **97**, 203.
18 Michael Dreja, Wim Pyckhout-Hintzen, Holger Mays and Bernd Tieke, *Langmuir*, 1999, **15**, 391.

19 V. K. Aswal, S. De, P. S. Goyal and P. Thiyagaragan, *J. Phys. Chem. B*, 1998, **102**, 2469.

20 V. Schmitt, F. Schosseler and F. Lequeux, *Europhys. Lett.*, 1995, **30**, 31.

21 R. Oda, P. Panizza, M. Schmutz and F. Lequeux, *Langmuir*, 1997, **13**, 6407.

22 T. A. Camesano and R. Nagarajan, *Colloids Surf., A*, 2000, **167**, 165.

23 V. Rajagopalan, B. S. Valaulikar and B. A. Dasannacharya, *Physica B*, 1992, **180**, 525.

24 S. H. Chen, *Annu. Rev. Phys. Chem.*, 1986, **37**, 351.

25 J. B. Hayter and J. Penfold, *Colloid Polym. Sci.*, 1983, **261**, 1022.

26 J. B. Hayter and J. Penfold, *J. Mol. Phys.*, 1981, **42**, 109.

27 P. S. Goyal, B. A. Dasnnacharya, V. K. Kelkar, C. Manohar, K. S. Rao and B. S. Valaulikar, *Physica B*, 1991, **174**, 196.

28 P. S. Goyal, *Phase Transitions*, 1994, **50**, 143.